Electronic correlations and magnetic interactions in infinite-layer $NdNiO_2$

Vamshi M. Katukuri,[1,*] Nikolay A. Bogdanov,[1] Oskar Weser,[1] Jeroen van den Brink,[2,3] and Ali Alavi[1,4,†]

[1] *Max Planck Institute for Solid State Research, Heisenbergstrasse 1, 70569 Stuttgart, Germany*
[2] *IFW Dresden, Helmholtzstrasse 20, 01069 Dresden, Germany*
[3] *Department of Physics, Technical University Dresden, Helmholtzstrasse 10, 01069 Dresden, Germany*
[4] *Department of Chemistry, University of Cambridge, Lensfield Road, Cambridge CB2 1EW, United Kingdom*

(Dated: November 6, 2021)

The large antiferromagnetic exchange coupling in the parent high-T_c cuprate superconductors is believed to play a crucial role in pairing the superconducting carriers. The recent observation of superconductivity in hole-doped infinite-layer (IL-) $NdNiO_2$ brings to the fore the relevance of magnetic coupling in high-T_c superconductors, particularly because no magnetic ordering is observed in the undoped IL-$NdNiO_2$ unlike in parent copper oxides. Here, we investigate the electronic structure and the nature of magnetic exchange in IL-$NdNiO_2$ using state-of-the-art many-body quantum chemistry methods. From a systematic comparison of the electronic and magnetic properties with isostructural cuprate IL-$CaCuO_2$, we find that the on-site dynamical correlations are significantly stronger in IL-$NdNiO_2$ compared to the cuprate analog. These dynamical correlations play a critical role in the magnetic exchange resulting in an unexpectedly large antiferromagnetic nearest neighbor isotropic J of 77 meV between the Ni^{1+} ions within the ab-plane. While we find many similarities in the electronic structure between the nickelate and the cuprate, the role of electronic correlations is profoundly different in the two. We further discuss the implications of our findings in understanding the origin of superconductivity in nickelates.

The recent discovery of superconductivity in hole-doped infinite layer (IL-) $NdNiO_2$ [1] marked a new direction in the efforts to understand the origin of high-T_c (hT_c)/unconventional superconductivity observed in strongly correlated materials. To date two classes of compounds have been discovered to exhibit the unconventional superconducting behavior – Copper oxides (cuprates) and iron based pnictides/chalcogenides (iron pnictides) with critical temperatures up to 134 K [2–4] and 46 K [5], respectively. Although a T_c of 15 K in $Nd_{0.8}Sr_{0.2}NiO_2$ [1] is rather low, the similarities in the crystal and electronic structures of the parent IL-$NdNiO_2$ with hT_c cuprate and iron-pnictide compounds, to a first approximation, renders their discovery remarkable. Particularly, it provides another play ground for a comparison of the essential physical features that may result in superconductivity.

While phonon mediated attraction is responsible for the formation of Cooper pairs in conventional superconductors [6] is long established, there is a large consensus that the most likely source of the electron gluing attractive potential in unconventional superconductors is provided by the antiferromagnetic (AF) correlations in the ground state (GS) [7–11]. It is proposed that the inherent strong quantum spin fluctuations take the role of "vibrations" analogous to phonons in conventional superconductors. The parent compounds of hT_c cuprates and pnictides are magnetically ordered with large AF exchange couplings (J). The highest nearest-neighbor (NN) J_1 of 250 meV is found in the cuprate Sr_2CuO_3 [12] with considerably smaller farther neighbor couplings [13]. On the other hand, both NN J_1 and next-nearest neighbor (NNN) J_2 interactions play a vital role in iron pnictides with $J_2 > J_1/2$ [14].

The IL-$NdNiO_2$ crystallizes in the $P4/mmm$ space-group and is iso-structural to IL-$CaCuO_2$ [15]. There are four oxygen atoms surrounding a nickel atom in a square-planar coordination and the rare-earth neodymium sits in the center of a cuboid formed by eight oxygens [see Figs 1(a) and 1(b)]. A formal +1 oxidation of Ni in IL-$NdNiO_2$ constitutes a strikingly similar valence $3d$-manifold as in the Cu^{2+} in cuprate superconductors, where a single hole is localized on the $3d_{x^2-y^2}$ orbital. However, no magnetic ordering is found in IL-$NdNiO_2$ [16], posing questions on the importance of magnetic correlations in the superconducting behavior in IL-$Nd_{0.8}Sr_{0.2}NiO_2$ [17]. A number of electronic structure calculations based on density functional theory (DFT) have shown that Ni $3d_{x^2-y^2}$ states sit at the Fermi energy level [18–20], with a significant overlap with Nd^{3+}

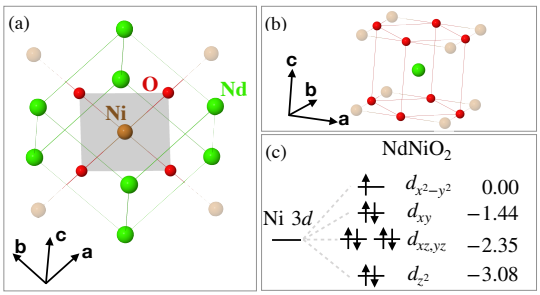

FIG. 1. (a) Square planar NiO_4 plaque and (b) the oxygen environment around the Nd^{3+} in IL-$NdNiO_2$. (c) Crystal field levels of the Ni^{1+} as computed from our calculations, and the energies in eV are also shown.

$5d$ states. It is argued that this close proximity of Nd $5d$ states results in a self-doping effect which reduces the Ni d-orbital occupancy to below 9. However, recent Nd M-edge x-ray absorption spectroscopic measurements [21] suggest that Nd remains in the +3 valence state, indicating the robustness of +1 oxidation of Ni. Based on the hopping matrix elements derived from DFT band structure calculations, it has been concluded that the magnetic interactions between Ni^{1+} ions are much smaller than in cuprates, $\approx$ 10 meV [19]. Further, a number of models have been explored based on one-, two- and multi-band Hamiltonians to derive the superconducting properties [17, 19, 20, 22–26]. Nonetheless, the lack of a reliable many-body description of the electronic structure of IL-$NdNiO_2$ renders it difficult to gauge the importance of different degrees of freedom and design pertinent investigative models to probe the origin of unconventional superconductivity.

In this work, in an effort to resolve this situation, we adopt many-body *ab initio* calculations to address the following three questions: (1) Is the electronic GS of the parent IL-$NdNiO_2$ similar to the one in parent hT_c superconducting cuprates? (2) How do the electronic correlations in IL-$NdNiO_2$ compare with those in IL-$CaCuO_2$? and (3) How strong is the magnetic exchange? To address these fundamental questions, we compute the electronic structure of the Ni^{1+} ions in the NiO_2 planes, particularly the Ni d-level multiplet structure using state-of-the-art wavefunction quantum chemistry methods. We quantify the electronic correlations among the valence and virtual orbitals, by computing the entanglement entropy, and unravel the similarities/differences in the electron interactions in the Ni and Cu compounds. Intriguingly, we find the on-site dynamical correlation is much stronger in IL-$NdNiO_2$ compared to IL-$CaCuO_2$. While we predict an AF Heisenberg J of 77 meV in IL-$NdNiO_2$, the J of 208 meV we compute for IL-$CaCuO_2$ is very close to $\approx$187 meV that is derived from the resonant inelastic x-ray scattering (RIXS) experiment [27].

d-orbital excitations. In Table I the relative energies of the d-orbital excitations obtained from multireference calculations for IL-$NdNiO_2$ and isostructural IL-$CaCuO_2$ are shown (for structural details, see Refs. [16, 28, 29]). These are obtained from a cluster-in-an-embedding calculation. Here, the electronic structure of a (quantum-) cluster of atoms carved from the solid is computed with many-body wavefunction calculations, while the solid-state environment is represented by the classical electrostatic field, which is computed from a set of point charges fitted to reproduce the Madelung potential within the cluster [30]. We use a single NiO_4 (CuO_4) square plaque along with the nearest neighbor Ni (Cu) and Nd (Ca) ions in the quantum-cluster [see Supplemental Material (SM) [31]] for the basis-set information and other computational details, which includes Refs. [32–53]

A combination of post Hartree-Fock (HF) complete active space self-consistent field (CASSCF) and multi-reference perturbation theory (MRPT) methods were employed to systematically capture the electron correlations [49]. A large active space consisting of five Ni (Cu) $3d$, all the O $2p$ orbitals of the NiO (CuO) plaque and the corresponding so-called "double-shell" orbitals (Ni (Cu) $4d$ and O $3p$) plus the semi-core Ni (Cu) $3s$ and unoccupied $4s$ orbitals, was considered, resulting in a 35 electrons in 36 orbitals – CAS(35,36)SCF – correlated calculation. An approximate solver based on density matrix renormalization group (DMRG) theory [42] was used to solve the eigenvalue problem defined within this active space, as conventional deterministic solvers are incapable of handling the resulting large Hilbert spaces. The number of renormalized states (M) was set to 3000 to guarantee convergence of the total energies. We employed the PYSCF quantum chemistry package [57] for all the calculations.

TABLE I. Relative energies (in eV) of the crystal field split Ni $3d$ orbitals in IL-$NdNiO_2$ and isostructural IL-$CaCuO_2$ obtained from CASSCF and CASSCF+NEVPT2 calculations. NEVPT2 corresponds to the N-electron valence perturbation theory [54, 55]. Excitation energies derived from RIXS measurement on IL-$CaCuO_2$ are also shown.

Orbital	$NdNiO_2$		$CaCuO_2$		
Sym.	CASSCF	+NEVPT2	CASSCF	+NEVPT2	RIXS [56]
$d_{x^2-y^2}$	0.00	0.00	0.00	0.00	0.00
d_{xy}	1.38	1.44	1.43	1.70	1.64
d_{xz}	2.24	2.35	2.04	2.21	1.95
d_{yz}	2.24	2.35	2.04	2.21	1.95
d_{z^2}	3.03	3.08	2.61	2.73	2.65

Unlike other many-body computational schemes, our calculations do not use any *ad hoc* parameters to incorporate electron-electron interactions and provides techniques to systematically analyze electron correlation effects. Such *ab initio* calculations offer insights into the electronic structure of correlated solids and go substantially beyond standard density-functional approaches [e.g., see Refs. [58–61] for the $3d$ transition metal (TM) oxides and Refs. [32, 62–65] for $5d$ compounds]. The larger active spaces considered in the present work are at the limit of what can be achieved today, and allow us to not only capture all the static and large portions of dynamic correlations but also enable us to understand their significance.

The d-d excitation energies for IL-$NdNiO_2$ shown in Table I exhibit a similar structure to that of the Cu^{2+} ion in IL-$CaCuO_2$. Contrary to the commonly accepted crystal field picture for a square planar coordination [66], the out-of-plane d_{z^2} is considerably lower in energy compared to the degenerate $d_{xz,yz}$ levels, as it is in IL-$CaCuO_2$. The excitation energies we compute for IL-$CaCuO_2$ reasonably fit with the peak positions in the RIXS spectrum [56] and previous calculations [59]. For IL-$NdNiO_2$,

the crystal field energy splittings we obtain are grossly different from those extracted from Wannier functions derived from band structure calculations [26], evidently displaying the crucial nature of many-body interactions. A significant difference in the multiplet structure of IL-$NdNiO_2$ and IL-$CaCuO_2$ is that the excitations into out-of-plane $d_{xz,yz}$- and d_{z^2}-like orbitals are $\approx$0.4 eV higher in the former. This is a consequence of the presence of bigger Nd^{3+} ions that increase the c-axis lattice parameter in IL-$NdNiO_2$, 3.28 Å (3.17 Å in IL-$CaCuO_2$), which further stabilize the out-of-plane orbitals.

To obtain insights into the electronic correlations in the GS of the two compounds, we analyzed their wavefunctions with the help of the full configuration interaction quantum Monte Carlo (FCIQMC) algorithm [67]. Using spin-adapted FCIQMC [68] from the NECI computer program [69], the GS wavefunctions within the CAS(35,36) space can be represented as a linear combination of configuration state functions (CSFs) (see SM [31] for details). One hundred million walkers were used to converge the total energies to within 0.1 mHa of the DMRG energies. We find that the GS wavefunction of IL-$NdNiO_2$ is more multi-configurational compared to the IL-$CaCuO_2$ GS wavefunction. While the first 1000 CSFs constitute 92.3% weight to the wavefunction in IL-$NdNiO_2$, their contribution is 94.6% in IL-$CaCuO_2$. The first three terms of the wavefunctions for IL-$NdNiO_2$ (NNO) and IL-$CaCuO_2$ (CCO), respectively, expressed in hole excitations from the reference (first) CSF [the subscript corresponds to the natural orbital numbers shown in Figs. 2(b)-2(d)], are

$$\psi_{\rm GS}^{\rm NNO} = 0.890|{\downarrow_1}\rangle + 0.072|{\downarrow_2}{\uparrow\downarrow_1}\rangle + 0.068|{\square_3}\,{\downarrow_1}{\uparrow\downarrow_{21}}\rangle + ...$$
$$\psi_{\rm GS}^{\rm CCO} = 0.896|{\downarrow_1}\rangle + 0.131|{\downarrow_2}{\uparrow\downarrow_1}\rangle + 0.054|{\uparrow_3}\,{\downarrow_1}{\downarrow_{21}}\rangle + ...$$

respectively, where $\uparrow/\downarrow$, $\uparrow\downarrow$ and $\square$ represent singly occupied, doubly occupied, and empty orbital states, respectively. While $\approx$ 80% of the wavefunction is dominated by the CSF with a hole in the $3d_{x^2-y^2}$-like orbital in both compounds, the rest of the composition of the wavefunction is quite different. The contribution from the O $2p$ charge transfer CSF (second term) is considerably smaller in IL-$NdNiO_2$ $\approx$0.5%, whereas in IL-$CaCuO_2$ it is $\approx$ 1.7%, over three times larger. The third term indicates a strong dynamic correlation (double excitation) between the $3d_{z^2}$- and $4d_{z^2}$-like orbitals in the Ni compound, whereas a single excitation (orbital relaxation) with a smaller weight in the Cu compound.

Electronic correlations. To further analyze the wavefunctions of the two compounds, we compute the entanglement entropy in them. When a wavefunction ($|\psi\rangle$) is represented in a Slater determinant/CSF basis, the electron correlation effects can be quantified by measuring the interaction between any pair of orbitals in which the electrons reside. Starting from the reduced density matrices (RDMs) corresponding to a wavefunction, computation of the von Neumann entropy of a particular orbital enables the quantification of electron correlations present in a quantum chemical system [46, 70, 71]. The single orbital entropy, $s(1)_i = -\sum_\mu w_{\mu,i} \ln w_{\mu,i}$, quantifies the correlation between the ith ($|\mathbf{i}\rangle$) orbital and the remaining set of orbitals ($|\mathbf{n}\rangle$) contained in the wavefunction expansion. Here, $w_{\mu,i}$ are the eigenvalues of the one orbital RDM $\rho^{(1)}_{i_\alpha,i_\beta}$ [46] (see SM [31]). Note that $s(1)_i$ has a maximum value of $\ln 4 \approx 1.39$ when all the four possible occupations of an orbital are equally probable. Thus an orbital with a large $s(1)$ experiences strong charge fluctuations implying a strongly correlated orbital. The total quantum information encoded in the wavefunction described by an active space is $I_{tot} = \sum_i s(1)_i$ and indicates the level of correlation in the wavefunction. The mutual information, $I_{i,j} = s(2)_{i,j} - s(1)_i - s(1)_j$, where $s(2)_{i,j}$ is the two-orbital entropy between i and j, [72, 73] illustrates the correlation of an orbital with another, in the embedded environment comprising all other orbitals. We used QCMAQUIS [74] and OPENMOLCAS [75] programs to compute the entropies.

In Fig. 2, $s(1)_i$ and $I_{i,j}$ computed from CAS(35,36)SCF RDMs for IL-$NdNiO_2$ and IL-$CaCuO_2$ are shown. From Figs. 2(a) and 2(c) we see $s(1) \gtrapprox 0.1$ for all the orbitals, implying their significant contribution to static (or non-dynamic) electron correlations. Typically, $s(1) \gtrapprox$

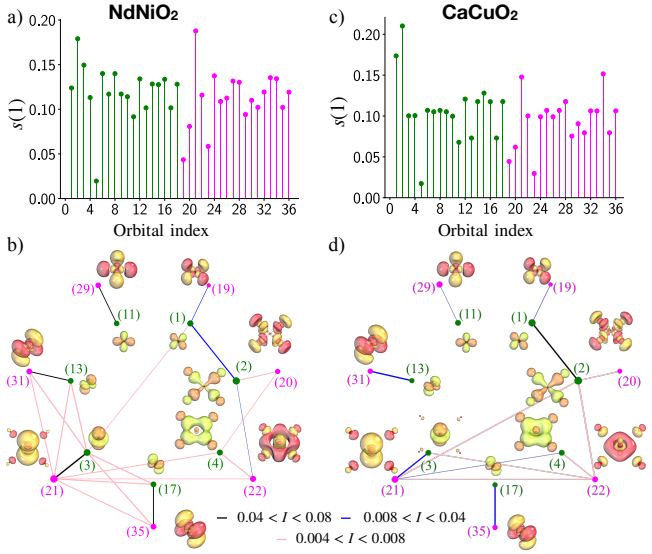

FIG. 2. (a) and (c) Single-orbital entropy, $s(1)_i$. (b) and (d) Mutual orbital information, $I_{i,j}$, between a few strongly entangled pairs of CASSCF natural orbitals (also shown) for IL-$NdNiO_2$ and IL-$CaCuO_2$, respectively. $I_{i,j}$ for all orbital pairs is shown in SM [31]. In (a) and (c) the green and magenta colors represent the two different set of orbitals, occupied (at the HF level) and the corresponding double-shell (virtual), respectively. The thicknesses of the black, blue and pink lines in (b) and (d) denote the strength of $I_{i,j}$, and the size of the dots is proportional to $s(1)_i$.

0.5 is observed for bonding-antibonding pairs and near-degenerate orbitals, signifying the multireference character of the wavefunction, whereas $s(1) \lessapprox 0.1$ is associated with orbitals important for dynamic correlations [70]. While $s(1)$ in a self-consistent natural orbital basis presents the entanglement between a more compact set of correlated orbitals, $s(1)$ in a self-consistent localized orbital basis also contains information about the orbital mixing in the self-consistent optimization of the orbital basis (see SM [31]).

The mutual information between pairs of orbitals plotted in Figs. 2(b) and 2(d) and Figs. S3 and S4 in SM [31] shows strong entanglement between the valence and their double-shell orbitals. Such strong entanglement is a result of dynamical (here mainly radial) correlation [49] and in the second-order the so-called "orbital breathing" effects that manifests when their occupation is allowed to change [76]. While, breathing of $3d$ orbitals has been studied earlier [76], it is interesting to find that radial correlations and breathing effects among O p orbitals are significant. An important observation here is the strong entanglement between Ni (Cu) $3d_{z^2}$- and $4d_{z^2}$-like orbitals. As we discuss below, this influences the exchange coupling in the two compounds. It can also be seen that the orbitals No. 1, – Ni (Cu) $3d_{x^2-y^2}$-like, and No. 2, – O $2p_\sigma$, are strongly entangled, which is the consequence of strong σ-type hybridization between the two, and which plays a crucial role in the magnetic exchange as well as the hole propagation when doped [77].

Now, let us compare the entropy information between IL-$NdNiO_2$ and IL-$CaCuO_2$. The total entanglement entropy contained in the GS wavefunction of $NdNiO_2$ (4.2) is larger than it is (3.6) for IL-$CaCuO_2$ indicating that the electron correlations are much more important/stronger in the former, an outcome of the greater multi-configurational character of the IL-$NdNiO_2$ GS wavefunction. Clearly, the radial-correlation and orbital breathing effects are much stronger in the nickel compound. A closer look at Fig. 2 reveals three major differences. (1) The Ni $3d_{z^2}$- and $4d_{z^2}$-like orbitals contribute rather significantly to the total entropy, in contrast to the Cu $3d_{z^2}$- and $4d_{z^2}$-like orbitals. Interestingly, we see a strong mixing of the Ni (Cu) $3d_{z^2}$ and $4s$ atomic-like orbitals in the CASSCF natural orbitals, however, this mixing is vastly different in Ni and Cu compounds (see Fig. S2 in SM [31] for the mutual information in the localized orbital basis). In IL-$NdNiO_2$ the Ni $4s$ atomic orbitals contribute significantly to the GS wavefunction. This corroborates with the recent reports of the Ni $4s$ orbital playing a crucial role in the self-doping effect caused by the Nd d manifold [24]. (2) The mutual information between the Ni $3d_{x^2-y^2}$- and O $2p_\sigma$-like orbitals indicates their hybridization is smaller than the corresponding Cu-O d-p hybridization, a key component for the superexchange. This difference would also influence the distribution of additional carriers upon doping. (3) In IL-$NdNiO_2$, mutual entropy between the Ni $3d_{z^2}$, $4d_{z^2}$ [orbitals No. (3,21)] and Ni $3d$ t_{2g} manifold [No. (13,31) and No. (17,35)] indicates the presence of dynamical angular-correlations as well, which incidentally are invisible (with the current scale) in IL-$CaCuO_2$.

Exchange interactions. The isotropic exchange J was extracted by mapping the low-energy spin spectrum of the two-magnetic-site cluster on to the Heisenberg model. The two-magnetic-site clusters we employed included two NiO_4 (CuO_4) square units, four neighboring Ni^{1+} (Cu^{2+}) ions, and all adjacent Nd^{3+} (Ca^{2+}) ions. To avoid the spin-couplings of the two central plaques with the neighboring Ni^{1+} (Cu^{2+}) ions we replaced them with closed-shell Cu^{1+} (Zn^{2+}) total ion potentials. See SM [31] for details. The spin-spectrum is computed within the CASSCF+MRPT formalism. The exchange in these systems is primarily of the superexchange type that depends on the virtual hopping of electrons (or holes) through the bridging oxygen and the effective on-site Coulomb repulsion (U_{eff}) on the $3d$ orbitals of the Ni (Cu) ions. To describe these two process accurately, it is essential to incorporate all the Ni (Cu) $3d$ and the corresponding double-shell $4d$ (10 + 10) orbitals as well as the bridging oxygen $2p$ and $3p$ (3 + 3) orbitals in the CASSCF active space. Specifically, it has been recently shown that the orbital breathing effects associated with $3d$–$4d$ single excitations are crucial [78]. On top of the CAS(24,26)SCF calculation, we performed multi-reference linearized coupled cluster (MRLCC) [52] calculations to capture the remaining correlation effects.

In Table II the computed exchange couplings are shown. The AF J that we compute for IL-$CaCuO_2$ is in good agreement with the experimental estimates of $J \approx 187$ meV [27]. However, in contrast to the recent reports of J an order of magnitude smaller in IL-$NdNiO_2$ compared to cuprates [17, 19], our calculations find a large nearest neighbor AF J of 77 meV in IL-$NdNiO_2$, close to half the size in IL-$CaCuO_2$. Given the reduced $3d_{x^2-y^2}$-$2p_\sigma$ hybridization due to larger d(Ni-O), evident in the GS wavefunction and the mutual entropy information, it might be surprising to find such large J. However, a subtle interplay of virtual hopping across the bridging oxygen and the effective on-site correlation U on Ni $3d$ orbitals is at play. While the decreased d-p hybridization reduces the virtual hopping across the bridging oxygen and lowers the superexchange, J is enhanced due to the

TABLE II. A comparison of the Heisenberg exchange couplings obtained from *ab initio* many-body calculations for IL-$NdNiO_2$ and IL-$CaCuO_2$. All values are given in meV. Positive values correspond to antiferromagnetic exchange.

	$NdNiO_2$		$CaCuO_2$	
	CASSCF	+MRLCC	CASSCF	+MRLCC
J	48.9	77.6	102.8	208.1

relatively smaller U in Ni compared to the U in Cu [79]. Additionally, the strong dynamical correlations we find in IL-$NdNiO_2$ further reduce the effective U significantly and increase the AF J.

It is remarkable that the $J = 48.9$ meV that we obtain at the CASSCF level is already about five times larger than $J \approx 10$ meV obtained when a reasonable value of on-site Coulomb repulsion ($U = 5$ eV) is plugged into the DFT+U calculations [19]. Note that J strongly varies with U and indeed for smaller U one obtains a J similar to what we compute [19]. While the CASSCF calculation includes the essential superexchange processes and the orbital relaxation effects associated with d^8-p^6-d^{10} and d^9-p^5-d^{10} configurations [80] in the superexchange mechanism [78], the MRLCC calculations capture all the dynamic correlations and polarization effects associated with the non-bridging oxygens and the farther atoms in the quantum-cluster. The latter calculation effectively renormalizes (decreases) the Coulomb interaction U on the Ni $3d$ orbitals, enhancing the J. Hybrid-DFT calculations estimate a J of 26 meV, more than two times larger than other DFT variants [20], reiterating the unreliability of DFT for estimating exchange couplings.

Discussion and conclusions. The superconducting phase in cuprates and iron-pnictides occurs in the proximity of the antiferromagnetically ordered state. Given the noticeable overall similarities of the electronic structure of IL-$NdNiO_2$ with an isostructural cuprate, and our finding of a significant exchange coupling persuade us to conclude that the superconducting state in hole-doped IL-$NdNiO_2$ is unconventional and is driven by AF fluctuations. One might argue that IL-$NdNiO_2$ is not antiferromagnetically ordered and hence the superconductivity is unlike in cuprates. It should be noted that the presence of AF correlations is of importance here but not an ordered state. There could be several possible reasons for the absence of AF ordering. It has been recently proposed that the GS of IL-$NdNiO_2$ could be close to a frustrated quantum critical point [81]. It has also been suggested that self-doping caused by the presence of Nd $5d$ states around the Fermi level can create a disordered magnetic lattice resulting in a quantum disordered state [82]. Indeed, it would be very interesting to see how doping would effect the GS of IL-$NdNiO_2$, given its multiconfigurational nature. Shall a hole be localized onto the O $2p$ states to form a Zhang-Rice singlet as in the cuprates [77] or is it accommodated on the Ni site? These questions we will address in a subsequent publication.

In conclusion, using state-of-the-art many-body configuration interaction calculations we have shown that the electronic structure of the parent IL-$NdNiO_2$ is similar to IL-$CaCuO_2$ but with noticeable differences. Primarily, the GS wavefunction is considerably more multiconfigurational in IL-$NdNiO_2$ with strong on-site dynamical correlations. These additional correlations considerably stabilize the singlet than the triplet resulting in an unexpectedly large AF J. With these findings we conclude that the superconductivity observed in IL d^9 nickelates is closely related to the superconductivity in d^9 cuprates, and a starting model Hamiltonian to investigate the superconductivity in IL-$NdNiO_2$ should consider the strong on-site dynamical correlations and effects of Ni $4s$ orbitals in addition to Ni $3d_{x^2-y^2}$ and O $2p$.

Note added in proof. The dd-exitation energies presented in Table 1 are in very good agreement with the recent RIXS measurements reported in Ref. [83].

V.M.K. acknowledges G. Li Manni for helping to get the best out of the OpenMolcas package and thank K. Guther and W. Dobrautz for promptly responding to queries on FCIQMC and NECI. V.M.K., N.A.B, O.W. and A.A. gratefully acknowledge funding from the Max Planck Society. J.v.d.B. is supported by the German Research Foundation (Deutsche Forschungsgemeinschaft) through the Würzburg-Dresden Cluster of Excellence on Complexity and Topology in Quantum Matter - ct.qmat (EXC 2147, project-id 39085490) and through SFB 1143 (project-id 247310070).

* V.Katukuri@fkf.mpg.de
† A.Alavi@fkf.mpg.de

[1] Danfeng Li, Kyuho Lee, Bai Yang Wang, Motoki Osada, Samuel Crossley, Hye Ryoung Lee, Yi Cui, Yasuyuki Hikita, and Harold Y. Hwang, "Superconductivity in an infinite-layer nickelate," Nature **572**, 624–627 (2019).
[2] J. G. Bednorz and K. A. Müller, "Possible high T-c superconductivity in the Ba-La-Cu-O system," Z. Phys. B **64**, 189 (1986).
[3] A. Schilling, M. Cantoni, J. D. Guo, and H. R. Ott, "Superconductivity above 130 K in the Hg-Ba-Ca-Cu-O system," Nature **363**, 56–58 (1993).
[4] Patrick A. Lee, Naoto Nagaosa, and Xiao-Gang Wen, "Doping a Mott insulator: Physics of high-temperature superconductivity," Rev. Mod. Phys. **78**, 17–85 (2006).
[5] Hiroki Takahashi, Kazumi Igawa, Kazunobu Arii, Yoichi Kamihara, Masahiro Hirano, and Hideo Hosono, "Superconductivity at 43 K in an iron-based layered compound $LaO_{1-x}F_xFeAs$," Nature **453**, 376–378 (2008).
[6] J. Bardeen, L. N. Cooper, and J. R. Schrieffer, "Microscopic Theory of Superconductivity," Phys. Rev. **106**, 162–164 (1957).
[7] P. W. Anderson, "The Resonating Valence Bond State in La_2CuO_4 and Superconductivity," Science **235**, 1196 (1987).
[8] Tôru Moriya and Kazuo Ueda, "Antiferromagnetic spin fluctuation and superconductivity," Rep. Prog. Phys. **66**, 1299–1341 (2003).
[9] P. W. Anderson, "PHYSICS: Is There Glue in Cuprate Superconductors?" Science **316**, 1705–1707 (2007).
[10] S. Sachdev, "Entangling Superconductivity and Antiferromagnetism," Science **336**, 1510–1511 (2012).
[11] B. Keimer, S. A. Kivelson, M. R. Norman, S. Uchida, and J. Zaanen, "From quantum matter to high-temperature superconductivity in copper oxides," Nature

518, 179–186 (2015).
[12] J. Schlappa, K. Wohlfeld, K. J. Zhou, M. Mourigal, M. W. Haverkort, V. N. Strocov, L. Hozoi, C. Monney, S. Nishimoto, S. Singh, A. Revcolevschi, J.-S. Caux, L. Patthey, H. M. Ronnow, J. van den Brink, and T. Schmitt, "Spin-orbital separation in the quasi-one-dimensional Mott insulator Sr_2CuO_3," Nature **485**, 82 (2012).
[13] R. Coldea, S. M. Hayden, G. Aeppli, T. G. Perring, C. D. Frost, T. E. Mason, S.-W. Cheong, and Z. Fisk, "Spin Waves and Electronic Interactions in La_2CuO_4," Phys. Rev. Lett. **86**, 5377–5380 (2001).
[14] Qimiao Si, Rong Yu, and Elihu Abrahams, "High-temperature superconductivity in iron pnictides and chalcogenides," Nat Rev Mater **1**, 16017 (2016).
[15] D. Di Castro, M. Salvato, A. Tebano, D. Innocenti, C. Aruta, W. Prellier, O. I. Lebedev, I. Ottaviani, N. B. Brookes, M. Minola, M. Moretti Sala, C. Mazzoli, P. G. Medaglia, G. Ghiringhelli, L. Braicovich, M. Cirillo, and G. Balestrino, "Occurrence of a high-temperature superconducting phase in $(CaCuO_2)_n/(SrTiO_3)_m$ superlattices," Phys. Rev. B **86**, 134524 (2012).
[16] M.A. Hayward and M.J. Rosseinsky, "Synthesis of the infinite layer Ni(I) phase $NdNiO_{2+x}$ by low temperature reduction of $NdNiO_3$ with sodium hydride," Solid State Sci. **5**, 839–850 (2003).
[17] Mi Jiang, Mona Berciu, and George A. Sawatzky, "Critical Nature of the Ni Spin State in Doped $NdNiO_2$," Phys. Rev. Lett. **124**, 207004 (2020).
[18] K.-W. Lee and W. E. Pickett, "Infinite-layer $LaNiO_2$: Ni^{1+} is not Cu^{2+}," Phys. Rev. B **70**, 165109 (2004).
[19] Zhao Liu, Zhi Ren, Wei Zhu, Zhengfei Wang, and Jinlong Yang, "Electronic and magnetic structure of infinite-layer $NdNiO_2$: trace of antiferromagnetic metal," npj Quantum Mater. **5**, 31 (2020).
[20] Hu Zhang, Lipeng Jin, Shanmin Wang, Bin Xi, Xingqiang Shi, Fei Ye, and Jia-Wei Mei, "Effective Hamiltonian for nickelate oxides $Nd_{1-x}Sr_xNiO_2$," Phys. Rev. Research **2**, 013214 (2020).
[21] Berit H. Goodge, Danfeng Li, Motoki Osada, Bai Yang Wang, Kyuho Lee, George A. Sawatzky, Harold Y. Hwang, and Lena F. Kourkoutis, "Doping evolution of the Mott-Hubbard landscape in infinite-layer nickelates," arXiv:2005.02847 [cond-mat] (2020).
[22] Hirofumi Sakakibara, Hidetomo Usui, Katsuhiro Suzuki, Takao Kotani, Hideo Aoki, and Kazuhiko Kuroki, "Model construction and a possibility of cuprate-like pairing in a new d^9 nickelate superconductor (Nd,Sr)NiO_2," arXiv:1909.00060 [cond-mat] (2019).
[23] Jonathan Karp, Antia S. Botana, Michael R. Norman, Hyowon Park, Manuel Zingl, and Andrew Millis, "Many-body Electronic Structure of $NdNiO_2$ and $CaCuO_2$," arXiv:2001.06441 [cond-mat] (2020).
[24] Priyo Adhikary, Subhadeep Bandyopadhyay, Tanmoy Das, Indra Dasgupta, and Tanusri Saha-Dasgupta, "Orbital Selective Superconductivity in a Two-band Model of Infinite-Layer Nickelates," arXiv:2005.01243 [cond-mat, physics:quant-ph] (2020).
[25] Motoharu Kitatani, Liang Si, Oleg Janson, Ryotaro Arita, Zhicheng Zhong, and Karsten Held, "Nickelate superconductors – a renaissance of the one-band Hubbard model," arXiv:2002.12230 [cond-mat] (2020).
[26] Xianxin Wu, Domenico Di Sante, Tilman Schwemmer, Werner Hanke, Harold Y. Hwang, Srinivas Raghu, and Ronny Thomale, "Robust $d_{x^2-y^2}$ -wave superconductivity of infinite-layer nickelates," Phys. Rev. B **101**, 060504 (2020).
[27] Y. Y. Peng, G. Dellea, M. Minola, M. Conni, A. Amorese, D. Di Castro, G. M. De Luca, K. Kummer, M. Salluzzo, X. Sun, X. J. Zhou, G. Balestrino, M. Le Tacon, B. Keimer, L. Braicovich, N. B. Brookes, and G. Ghiringhelli, "Influence of apical oxygen on the extent of in-plane exchange interaction in cuprate superconductors," Nat. Phys. **13**, 1201–1206 (2017).
[28] Naoya Kobayashi, Zenji Hiroi, and Mikio Takano, "Compounds and Phase Relations in the SrO-CaO-CuO System under High Pressure," J. Solid State Chem. **132**, 274–283 (1997).
[29] J. Karpinski, I. Mangelschots, H. Schwer, K. Conder, A. Morawski, T. Lada, and A. Paszewin, "Single crystal growth of HgBaCaCuO and infinite layer $CaCuO_2$ at high gas pressure," Physica C **235-240**, 917–918 (1994).
[30] P. P. Ewald, "Die Berechnung optischer und elektrostatischer Gitterpotentiale," Ann. Phys. **369**, 253–287 (1921).
[31] See Supplemental Material at the publisher website.
[32] Vamshi M. Katukuri, Hermann Stoll, Jeroen van den Brink, and Liviu Hozoi, "*Ab initio* determination of excitation energies and magnetic couplings in correlated quasi-two-dimensional iridates," Phys. Rev. B **85**, 220402 (2012).
[33] Vamshi M. Katukuri, Karla Roszeitis, Viktor Yushankhai, Alexander Mitrushchenkov, Hermann Stoll, Michel van Veenendaal, Peter Fulde, Jeroen van den Brink, and Liviu Hozoi, "Electronic Structure of Low-Dimensional 4dˆ5 Oxides: Interplay of Ligand Distortions, Overall Lattice Anisotropy, and Spin–Orbit Interactions," Inorg. Chem. **53**, 4833–4839 (2014).
[34] P. Babkevich, Vamshi M. Katukuri, B. Fåk, S. Rols, T. Fennell, D. Pajić, H. Tanaka, T. Pardini, R. R. P. Singh, A. Mitrushchenkov, O. V. Yazyev, and H. M. Rønnow, "Magnetic Excitations and Electronic Interactions in Sr_2CuTeO_6: A Spin-1/2 Square Lattice Heisenberg Antiferromagnet," Phys. Rev. Lett. **117**, 237203 (2016).
[35] M. Klintenberg, S.E. Derenzo, and M.J. Weber, "Accurate crystal fields for embedded cluster calculations," Comp. Phys. Comm. **131**, 120 (2000).
[36] Björn O. Roos, Roland Lindh, P. Malmqvist, Valera Veryazov, and P. Widmark, "New Relativistic ANO Basis Sets for Transition Metal Atoms," J. Phys. Chem. A **109**, 6575–6579 (2005).
[37] Björn O. Roos, Roland Lindh, P. Malmqvist, Valera Veryazov, and P. Widmark, "Main Group Atoms and Dimers Studied with a New Relativistic ANO Basis Set," J. Phys. Chem. A **108**, 2851–2858 (2004).
[38] M. Dolg, H. Stoll, A. Savin, and H. Preuss, "Energy-adjusted pseudopotentials for the rare earth elements," Theor. Chim. Acta **75**, 173–194 (1989).
[39] M. Dolg, H. Stoll, and H. Preuss, "A combination of quasirelativistic pseudopotential and ligand field calculations for lanthanoid compounds," Theor. Chim. Acta **85**, 441–450 (1993).
[40] M. Kaupp, P. v. R. Schleyer, H. Stoll, and H. Preuss, "Pseudopotential approaches to Ca, Sr, and Ba hydrides. Why are some alkaline earth MX_2 compounds bent?" J. Chem. Phys. **94**, 1360–1366 (1991).
[41] Gudrun Igel-Mann, *Semiempirische Pseudopotentiale:*

Untersuchungen an Hauptgruppenelementen und Nebengruppenelementen mit abgeschlossener d-Schale, Ph.D. thesis, Stuttgart, Univ., Stuttgart (1987).

[42] Sandeep Sharma and Garnet Kin-Lic Chan, "Spin-adapted density matrix renormalization group algorithms for quantum chemistry," J. Chem. Phys. **136**, 124121 (2012).

[43] Deidre Cleland, George H. Booth, and Ali Alavi, "Survival of the fittest: Accelerating convergence in full configuration-interaction quantum Monte Carlo," J. Chem. Phys. **132**, 041103 (2010).

[44] N. S. Blunt, Simon D. Smart, J. A. F. Kersten, J. S. Spencer, George H. Booth, and Ali Alavi, "Semi-stochastic full configuration interaction quantum Monte Carlo: Developments and application," J. Chem. Phys. **142**, 184107 (2015).

[45] Khaldoon Ghanem, Alexander Y. Lozovoi, and Ali Alavi, "Unbiasing the initiator approximation in full configuration interaction quantum Monte Carlo," J. Chem. Phys. **151**, 224108 (2019).

[46] Katharina Boguslawski and Paweł Tecmer, "Orbital entanglement in quantum chemistry," Int. J. Quantum Chem. **115**, 1289–1295 (2015).

[47] Thom H. Dunning Jr., "Gaussian basis sets for use in correlated molecular calculations. I. The atoms boron through neon and hydrogen," J. Chem. Phys. **90**, 1007–1023 (1989).

[48] Nikolai B. Balabanov and Kirk A. Peterson, "Systematically convergent basis sets for transition metals. I. All-electron correlation consistent basis sets for the 3d elements Sc-Zn," J. Chem. Phys. **123**, 064107 (2005).

[49] T. Helgaker, P. Jørgensen, and J. Olsen, *Molecular electronic-structure theory* (Wiley, Chichester, 2000).

[50] Kerstin Andersson, PerÅke Malmqvist, and Björn O. Roos, "Second-order perturbation theory with a complete active space self-consistent field reference function," J. Chem. Phys. **96**, 1218–1226 (1992).

[51] Kenneth G. Dyall, "The choice of a zeroth-order Hamiltonian for second-order perturbation theory with a complete active space self-consistent-field reference function," J. Chem. Phys. **102**, 4909–4918 (1995).

[52] Sandeep Sharma and Ali Alavi, "Multireference linearized coupled cluster theory for strongly correlated systems using matrix product states," J. Chem. Phys. **143**, 102815 (2015).

[53] Reinhold F. Fink, "Two new unitary-invariant and size-consistent perturbation theoretical approaches to the electron correlation energy," Chem. Phys. Lett. **428**, 461 – 466 (2006).

[54] C. Angeli, R. Cimiraglia, and J.-P. Malrieu, "N-electron valence state perturbation theory: a fast implementation of the strongly contracted variant," Chem. Phys. Lett. **350**, 297 (2001).

[55] Sandeep Sharma, Gerald Knizia, Sheng Guo, and Ali Alavi, "Combining Internally Contracted States and Matrix Product States To Perform Multireference Perturbation Theory," J. Chem. Theory Comput. **13**, 488–498 (2017).

[56] M Moretti Sala, V Bisogni, C Aruta, G Balestrino, H Berger, N B Brookes, G M de Luca, D Di Castro, M Grioni, M Guarise, P G Medaglia, F Miletto Granozio, M Minola, P Perna, M Radovic, M Salluzzo, T Schmitt, K J Zhou, L Braicovich, and G Ghiringhelli, "Energy and symmetry of dd excitations in undoped layered cuprates measured by Cu L_3 resonant inelastic x-ray scattering," New J. Phys. **13**, 043026 (2011).

[57] Qiming Sun, Timothy C. Berkelbach, Nick S. Blunt, George H. Booth, Sheng Guo, Zhendong Li, Junzi Liu, James D. McClain, Elvira R. Sayfutyarova, Sandeep Sharma, Sebastian Wouters, and Garnet Kin-Lic Chan, "PySCF: the Python-based simulations of chemistry framework," WIREs Comput. Mol. Sci. **8**, e1340 (2017).

[58] D. Muñoz, F. Illas, and I. de P. R. Moreira, "Accurate Prediction of Large Antiferromagnetic Interactions in High-T_c $HgBa_2Ca_{n-1}Cu_nO_{2n+2+\delta}$ (n=2,3) Superconductor Parent Compounds," Phys. Rev. Lett. **84**, 1579–1582 (2000).

[59] L. Hozoi, L. Siurakshina, P. Fulde, and J. van den Brink, "Ab initio determination of cu 3d orbital energies in layered copper oxides," Sci. Rep. **1**, 65 (2011).

[60] L. Hozoi and P.Fulde, *Computational Methods for Large Systems: Electronic Structre Approaches for Biotechnology and Nanotechnology* (John Wiley & Sons, Hoboken, 2011) Chap. 6.

[61] N. A. Bogdanov, J. van den Brink, and L. Hozoi, "*Ab initio* computation of *d-d* excitation energies in low-dimensional Ti and V oxychlorides," Phys. Rev. B **84**, 235146 (2011).

[62] Nikolay A. Bogdanov, Rémi Maurice, Ioannis Rousochatzakis, Jeroen van den Brink, and Liviu Hozoi, "Magnetic State of Pyrochlore $Cd_2Os_2O_7$ Emerging from Strong Competition of Ligand Distortions and Longer-Range Crystalline Anisotropy," Phys. Rev. Lett. **110**, 127206 (2013).

[63] H. Gretarsson, J. P. Clancy, X. Liu, J. P. Hill, Emil Bozin, Yogesh Singh, S. Manni, P. Gegenwart, Jungho Kim, A. H. Said, D. Casa, T. Gog, M. H. Upton, Heung-Sik Kim, J. Yu, Vamshi M. Katukuri, L. Hozoi, J. van den Brink, and Young-June Kim, "Crystal-Field Splitting and Correlation Effect on the Electronic Structure of A_2IrO_3," Phys. Rev. Lett. **110**, 076402 (2013).

[64] Vamshi M. Katukuri, Viktor Yushankhai, Liudmila Siurakshina, Jeroen van den Brink, Liviu Hozoi, and Ioannis Rousochatzakis, "Mechanism of basal-plane antiferromagnetism in the spin-orbit driven iridate ba_2iro_4," Phys. Rev. X **4**, 021051 (2014).

[65] V. M Katukuri, S. Nishimoto, V. Yushankhai, A. Stoyanova, H. Kandpal, S. Choi, R. Coldea, I. Rousochatzakis, L. Hozoi, and J. van den Brink, "Kitaev interactions between $j = 1/2$ moments in honeycomb Na_2IrO_3 are large and ferromagnetic: insights from ab initio quantum chemistry calculations," New J. Phys. **16**, 013056 (2014).

[66] E A Moore and Rob Janes, eds., "Metal-Ligand Bonding," (The Royal Society of Chemistry, 2004) Chap. Substitute and Distorted Octahedral Complexes, and Square-planar Complexes, pp. 21–27.

[67] George H. Booth, Alex J. W. Thom, and Ali Alavi, "Fermion Monte Carlo without fixed nodes: a game of life, death, and annihilation in Slater determinant space," J. Chem. Phys. **131**, 054106 (2009).

[68] Werner Dobrautz, Simon D. Smart, and Ali Alavi, "Efficient formulation of full configuration interaction quantum Monte Carlo in a spin eigenbasis via the graphical unitary group approach," J. Chem. Phys. **151**, 094104 (2019).

[69] K. Guther, R. J. Anderson, N. S. Blunt, N. A. Bogdanov, D. Cleland, D. Dattani, W. Dobrautz, K. Ghanem,

P. Jeszenski, N. Liebermann, G. Li Manni, A. Y. Lozovoi, H. Luo, D. Ma, F. Merz, C. Overy, M. Rampp, P. K. Samanta, L. R. Schwarz, J. J. Shepherd, S. D. Smart, E. Vitale, O. Weser, G. H. Booth, and A. Alavi, "NECI: N-Electron Configuration Interaction with an emphasis on state-of-the-art stochastic methods," J. Chem. Phys. **153**, 034107 (2020).

[70] Katharina Boguslawski, Paweł Tecmer, Örs Legeza, and Markus Reiher, "Entanglement Measures for Single and Multireference Correlation Effects," J. Phys. Chem. Lett. **3**, 3129–3135 (2012).

[71] Katharina Boguslawski, Paweł Tecmer, Gergely Barcza, Örs Legeza, and Markus Reiher, "Orbital Entanglement in Bond-Formation Processes," J. Chem. Theory Comput. **9**, 2959–2973 (2013).

[72] J. Legeza and J. Sölyom, "Optimizing the density-matrix renormalization group method using quantum information entropy," Phys. Rev. B **68**, 195116 (2003).

[73] Jörg Rissler, Reinhard M. Noack, and Steven R. White, "Measuring orbital interaction using quantum information theory," Chemical Physics **323**, 519–531 (2006).

[74] Sebastian Keller, Michele Dolfi, Matthias Troyer, and Markus Reiher, "An efficient matrix product operator representation of the quantum chemical Hamiltonian," J. Chem. Phys. **143**, 244118 (2015).

[75] Ignacio Fdez. Galván, Morgane Vacher, Ali Alavi, Celestino Angeli, Francesco Aquilante, Jochen Autschbach, Jie J. Bao, Sergey I. Bokarev, Nikolay A. Bogdanov, Rebecca K. Carlson, Liviu F. Chibotaru, Joel Creutzberg, Nike Dattani, Mickaël G. Delcey, Sijia S. Dong, Andreas Dreuw, Leon Freitag, Luis Manuel Frutos, Laura Gagliardi, Frédéric Gendron, Angelo Giussani, Leticia González, Gilbert Grell, Meiyuan Guo, Chad E. Hoyer, Marcus Johansson, Sebastian Keller, Stefan Knecht, Goran Kovačević, Erik Källman, Giovanni Li Manni, Marcus Lundberg, Yingjin Ma, Sebastian Mai, João Pedro Malhado, PerÅke Malmqvist, Philipp Marquetand, Stefanie A. Mewes, Jesper Norell, Massimo Olivucci, Markus Oppel, Quan Manh Phung, Kristine Pierloot, Felix Plasser, Markus Reiher, Andrew M. Sand, Igor Schapiro, Prachi Sharma, Christopher J. Stein, Lasse Kragh Sørensen, Donald G. Truhlar, Mihkel Ugandi, Liviu Ungur, Alessio Valentini, Steven Vancoillie, Valera Veryazov, Oskar Weser, Tomasz A. Wesołowski, Per-Olof Widmark, Sebastian Wouters, Alexander Zech, J. Patrick Zobel, and Roland Lindh, "OpenMolcas: From Source Code to Insight," J. Chem. Theory Comput. **15**, 5925–5964 (2019).

[76] O. Gunnarsson, O. K. Andersen, O. Jepsen, and J. Zaanen, "Density-functional calculation of the parameters in the Anderson model: Application to Mn in CdTe," Phys. Rev. B **39**, 1708 (1989).

[77] F. C. Zhang and T. M. Rice, "Effective Hamiltonian for the superconducting Cu oxides," Phys. Rev. B **37**, 3759–3761 (1988).

[78] Nikolay A. Bogdanov, Giovanni Li Manni, Sandeep Sharma, Olle Gunnarsson, and Ali Alavi, "New superexchange paths due to breathing-enhanced hopping in corner-sharing cuprates," arXiv:1803.07026 [cond-mat] (2018).

[79] Kazuma Nakamura, Ryotaro Arita, Yoshihide Yoshimoto, and Shinji Tsuneyuki, "First-principles calculation of effective onsite Coulomb interactions of 3d transition metals: Constrained local density functional approach with maximally localized Wannier functions," Phys. Rev. B **74**, 235113 (2006).

[80] Daniel I. Khomskii, *Transition Metal Compounds* (Cambridge University Press, 2014).

[81] Mi-Young Choi, W. E. Pickett, and K.-W. Lee, "Quantum-Fluctuation-Frustrated Flat Band Instabilities in $NdNiO_2$," arXiv:2005.03234 [cond-mat] (2020).

[82] Kazuki Uematsu and Hikaru Kawamura, "Randomness-induced quantum spin liquid behavior in the $s = 1/2$ random J_1 - J_2 Heisenberg antiferromagnet on the square lattice," Phys. Rev. B **98**, 134427 (2018).

[83] M. Rossi, H. Lu, A. Nag, D. Li, M. Osada, K. Lee, B. Y. Wang, S. Agrestini, M. Garcia-Fernandez, Y. D. Chuang, Z. X. Shen, H. Y. Hwang, B. Moritz, Ke-Jin Zhou, T. P. Devereaux, and W. S. Lee, "Orbital and Spin Character of Doped Carriers in Infinite-Layer Nickelates," (2020), arXiv:2011.00595 [cond-mat.str-el].